J Mater Sci (2011) 46:4622–4629
DOI 10.1007/s10853-011-5364-4

On the thermal stability of the copper–titanium–zirconium phosphate solid-solution series: $CuTi_{2-x}Zr_x(PO_4)_3$ ($0 \leq x \leq 2$) under air

T. E. Warner · E. M. Skou

Received: 15 December 2010 / Accepted: 31 January 2011 / Published online: 18 February 2011
© Springer Science+Business Media, LLC 2011

Abstract The solid copper(I) electrolytes: $CuTi_2(PO_4)_3$; $CuTiZr(PO_4)_3$; and $CuZr_2(PO_4)_3$; were prepared as powders by high temperature synthesis and analysed by powder XRD. These materials were then annealed in air at 400 °C for 72 h. The results of powder XRD showed that the degree of oxidation under these conditions varies progressively and enormously across this series, with the passivity dependent upon the Ti/Zr ratio; $CuTi_2(PO_4)_3$ being the least reactive under these conditions. The results of the thermogravimetric analyses in artificial air ($P_{O_2} = 0.2$ bar) corroborate with the above, and reveal in all cases that $T_{eqm} = 500 \pm 25$ °C for the reversible reaction: $4Cu\,(Ti, Zr)_2(PO_4)_3 + O_2 \leftrightarrows 4Cu_{0.5}\,(Ti, Zr)_2(PO_4)_3 + 2CuO$. Green $Cu_{0.5}TiZr\,(PO_4)_3$ has been prepared as a new compound and was shown to belong to a rhombohedral system with hexagonal cell constants: $a = 8.599(1)$ Å; $c = 22.355(3)$ Å; $Z = 6$.

Introduction

The solid-solution series $CuTi_{2-x}Zr_x(PO_4)_3$ ($0 \leq x \leq 2$) crystallizes with the NASICON-type structure; NASICON being an acronym for the *Na-superionic conductor* in reference to $Na_{1+x}Zr_2(SiO_4)_x(PO_4)_{3-x}$ ($0 \leq x \leq 3$) [1]. This is essentially a three-dimensional open-framework structure that allows for fast copper(I) ion conduction at elevated temperature. The copper containing material is often referred to by the analogous acronym, CUSICON; *Cu-superionic* conductor [2]. The crystal structure of $CuTi_2(PO_4)_3$ and its copper(II) analogue, $Cu_{0.5}Ti_2(PO_4)_3$, are shown in Figs. 1 and 2, respectively. With regard to the end-members: $CuZr_2(PO_4)_3$ has been used as a solid electrolyte in electrochemical sensors [3]; whilst, $CuTi_2(PO_4)_3$ has been used as a heterogeneous catalyst for the oxidation of propene to acrolein [4, 5].

$CuZr_2(PO_4)_3$ was prepared originally by Yao and Fray in 1983 [2]; stoichiometric amounts of Cu_2O, ZrO_2 and $NH_4H_2PO_4$ were milled together for 16 h, then heated to 300 °C for 4 h in order to decompose the $NH_4H_2PO_4$, before calcining at 850 °C in air for 16 h. The partially sintered mixture was ground and pressed isostatically into monoliths. These were then heated in air to 1,200 °C for ~5 h before cooling to ambient temperature. The titanium analogue, $CuTi_2(PO_4)_3$ was prepared originally by Mbandza et al. [6] in 1985, by a similar high temperature method. Single phase material was prepared successfully, whilst deploying a notably lower reaction temperature of 850 °C.

The midintermediate member, $CuTiZr(PO_4)_3$ was discovered subsequently, using different reaction routes by, Berry et al. [7] and Warner et al. [8], in 1992. Berry et al. [7] prepared $CuTiZr(PO_4)_3$ by reacting together an appropriate mixture of Cu_2O, TiO_2 (anatase), ZrO_2 and $NH_4H_2PO_4$ at 300 °C for 3 h in air. This material was re-ground and heated at 1,200 °C for 36 h in air. The product material, $CuTiZr(PO_4)_3$ was described as pale brown. Warner et al. [8] prepared $CuTiZr(PO_4)_3$ by sintering an equimolar mixture of $CuTi_2(PO_4)_3$ and $CuZr_2(PO_4)_3$, at 1,300 °C for 16 h under a flowing atmosphere of argon. Powder X-ray diffractometry indicated that this material comprised a wide range of solid-solution compositions, $CuTi_{2-x}Zr_x(PO_4)_3$ ($0 \leq x \leq 2$). The homogeneous composition $CuTiZr(PO_4)_3$ was obtained eventually, with an

T. E. Warner (✉) · E. M. Skou
Institute of Chemical Engineering, Biotechnology and Environmental Technology, University of Southern Denmark, Niels Bohrs Allé 1, 5230 Odense M, Denmark
e-mail: tew@kbm.sdu.dk

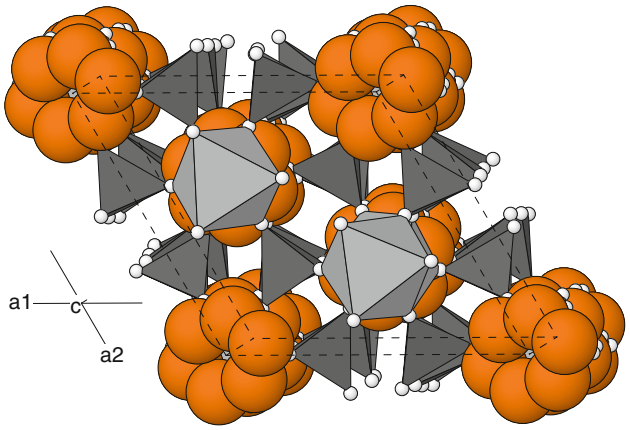

Fig. 1 Crystal structure of $CuTi_2(PO_4)_3$ emphasising the six off-centred equivalent positions in the M(1) site (*shown as large orange spheres*) which are partially occupied by the Cu^+ ions; site occupation factor = 1/6. The distorted nature of these copper sites appear like 'daisy-heads' running parallel to the *a*1-*a*2 basal plane. The trigonal unit cell (*drawn in dash*) corresponds to the usual hexagonal coordinates as viewed here down the *c*-axis. This figure was drawn using data from Mbandza et al. [21] cf. ICSD 68322

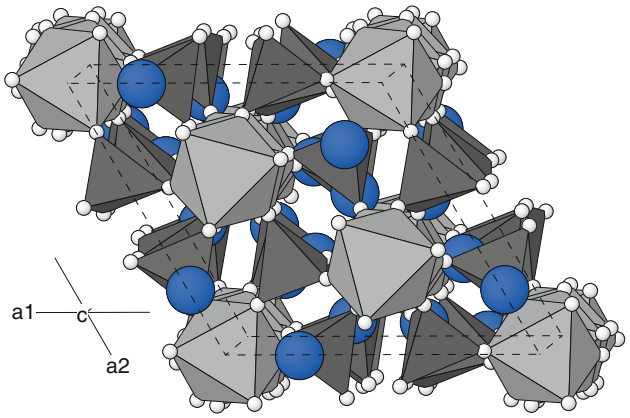

Fig. 2 Crystal structure of $Cu_{0.5}Ti_2(PO_4)_3$ emphasising the M(2) site (*shown as large blue spheres*) which are partially occupied by the Cu^{2+} ions; site occupation factor = 1/6. The trigonal unit cell (*drawn in dash*) corresponds to the usual hexagonal coordinates as viewed here down the *c*-axis. This figure was drawn using data from Olazcuaga et al. [19] cf. ICSD 81253

orange colouration, after regrinding and sintering a newly compacted charge.

The end-members, $CuTi_2(PO_4)_3$ and $CuZr_2(PO_4)_3$, have been oxidised under an atmosphere of flowing oxygen at 500 °C, yielding the blue-green copper(II) analogue phases, $Cu_{0.5}Ti_2(PO_4)_3$ [9] and $Cu_{0.5}Zr_2(PO_4)_3$ [10]. In the case of $CuZr_2(PO_4)_3$, Le Polles et al. [11] mentioned that complete oxidation is achieved within 15 h. Pertinent to this present work, is that no comment is made in the literature as to the length of time that is required to afford a complete oxidation of the titanium compound, $CuTi_2(PO_4)_3$. However, $Cu_{0.5}Ti_2(PO_4)_3$ and $Cu_{0.5}Zr_2(PO_4)_3$ were reported to undergo a reversible allotropic transition from monoclinic to rhombohedral at 550 and 520 °C, respectively [9, 10]. Furthermore, $Cu_{0.5}Zr_2(PO_4)_3$ has also been prepared in a more direct fashion, by two different sol–gel routes, with subsequent annealing at ~800 °C [12, 13].

The possibility of forming a solid solution between $CuZr_2(PO_4)_3$ and $Cu_{0.5}Zr_2(PO_4)_3$ was a controversial issue for many years. Stoichiometric $CuZr_2(PO_4)_3$ can be prepared as a white powder [8, 14], but this phase often displays various shades of pale-green, which indicates the presence of copper(II) in the solid state. Recently, Christensen et al. [15] performed an electron paramagnetic resonance study of the $CuZr_2(PO_4)_3$–$Cu_{0.5}Zr_2(PO_4)_3$ system, and concluded that $Cu_{1-\delta}Zr_2(PO_4)_3$ does contain Cu^{2+} ions, but only at a dilute ($\delta << 0.5$) and dispersed level of concentration. Thus, the extent of any solid solution between $CuZr_2(PO_4)_3$ and $Cu_{0.5}Zr_2(PO_4)_3$ was found to be very limited. Christensen et al. [15] suggested that the local distortions exerted by the very different coordination of the Cu^+ and Cu^{2+} ions—upon the otherwise very similar $[Zr_2(PO_4)_3]^-$ structural framework—may be too extreme for this material to accommodate these ions simultaneously; besides that at a defect level of concentration.

In the course of preparing these materials over many years (as a laboratory exercise for students), it has become apparent that $CuTi_2(PO_4)_3$ and $CuZr_2(PO_4)_3$ display certain differences in the ease with which they can be prepared. Ceramic $CuTi_2(PO_4)_3$ can be prepared quite readily from its constituent oxides at 850 °C in air, and remains apparently in its reduced state throughout the normal furnace cooling rate of about 300 °C/h. Conversely, the preparation of ceramic $CuZr_2(PO_4)_3$ from its constituent oxides, demands a reaction temperature of at least 1,150 °C [16]. Furthermore, $CuZr_2(PO_4)_3$ is much more susceptible to oxidation during the cooling process. Warner et al. [16] and Christensen et al. [15] have shown that $CuZr_2(PO_4)_3$ becomes oxidised when cooled in air during normal furnace cooling rates; yielding a mottled dark green-grey material. The preparation of $CuZr_2(PO_4)_3$ demands that the product material is either quenched in air from ~700 °C, or allowed to cool at more moderate rates whilst under a protective inert atmosphere, such as, argon.

In this present article, we report our findings from a study of the relative thermal stabilities of $CuTi_2(PO_4)_3$, $CuTiZr(PO_4)_3$, and $CuZr_2(PO_4)_3$ under air (P_{O_2} = 0.2 bar). The results of the analyses by powder X-ray diffractometry on these materials, prior to and after oxidation, are compared with the corresponding set of results from thermogravimetry. The implications to the technological exploitation of these materials are discussed.

Experimental

Synthesis of $CuTi_2(PO_4)_3$; $CuTiZr(PO_4)_3$; and $CuZr_2(PO_4)_3$

10 g samples of each of the materials: $CuTi_2(PO_4)_3$; $CuTiZr(PO_4)_3$; and $CuZr_2(PO_4)_3$ were prepared by the following method: the appropriate amounts of copper(II) oxide (Aldrich 99+%); titanium(IV) oxide, rutile (Aldrich 99.9+% < 5 μm); zirconium(IV) oxide (Aldrich 99.9% < 1 μm); and ammonium dihydrogenphosphate (Aldrich 99.99+%) were ground together thoroughly in their dry state, using a porcelain pestle and mortar, then placed in an alumina crucible (CC62 Almath Ltd.) with its corresponding alumina lid. These were introduced into a chamber furnace (Lenton Furnaces UAF15/10) and heated in air at 60 °C/h to 300 °C. After 3 h at 300 °C, the temperature was raised at 200 °C/h to 1,250 °C. After 48 h at 1,250 °C, the material was cooled at 200 °C/h to ambient temperature. The intermediate product material was extracted from the crucible and ground to a fine powder using an agate pestle and mortar.

Ceramic monoliths of each of the above materials were fabricated by compressing $\sim$10 g of the above respective powders into a disc using a 32 mm diameter Specac stainless steel die and a uniaxial press with a load $\sim 1 \times 10^4$ kg. The compaction of the powder was performed in order to promote the solid-state reaction (that is dependent on solid-state diffusion processes), with the objective of yielding single phase material. These powder compacts were placed directly into an alumina boat (SRX110 Almath Ltd) and introduced into the central zone of a tube furnace (Lenton Furnaces LTF 16/50/180); then heated to 1,250 °C in air with a heating rate of 200 °C/h. After 55 h at 1,250 °C, the charge was then cooled to 700 °C with a cooling rate of 200 °C/h. Once at 700 °C, the 'red-hot' ceramic monoliths were removed from the furnace using a pair of steel forceps and plunged immediately into water in order to quench them; then retrieved from the water and dried using a warm air blower. The monoliths were then crushed and ground to a fine powder using an agate pestle and mortar. A sample ($\sim$1 g) of the powder was analysed by powder X-ray diffractometry (10–40° 2θ) using a Siemens D5000 powder diffractometer using Cu $K_{\alpha 1}$ radiation ($\lambda = 1.5405$ Å) with an associated data capture/treatment system. Where relevant, indexing of the respective powder patterns was performed using the software: *program for the automatic indexing of powder diffraction patterns by the successive dichotomy method* (DICVOL06) written by, Boultif and Louer [17].

Oxidation of $CuTi_2(PO_4)_3$; $CuTiZr(PO_4)_3$; and $CuZr_2(PO_4)_3$

Finely powered samples ($\sim$5 g) of the above materials were placed in three shallow alumina crucibles (LR42 Almath Ltd) and oxidised in air by placing them, simultaneously, inside a pre-heated chamber furnace held at 400 °C for 72 h, before cooling to ambient temperature at 200 °C/h. The product materials of this oxidation process were analysed by powder X-ray diffractometry.

An attempt to prepare single phase $Cu_{0.5}TiZr(PO_4)_3$ was conducted by the following method. Approximately 9 g of finely powdered $CuTiZr(PO_4)_3$ was spread evenly in an alumina boat (SRX110 Almath Ltd) and heated in a tube furnace under an atmosphere of flowing oxygen (500 ml/min at STP) at 400 °C for 48 h; with a heating and cooling rate of 200 °C/h. The product material was then ground and placed in a glass beaker, together with 100 ml of warm ($\sim$50 °C) 4 mol dm^{-3} HNO_3 acid solution in order to dissolve the exsolved copper oxide. This mixture was then filtered using a Buchner filter funnel. The powder bed was washed, first with distilled water, then ethanol, and finally left to dry. The final product material was analysed by powder X-ray diffraction.

Thermogravimetric analyses

Thermogravimetric analysis was performed on each of the following materials: 24.53 mg $CuZr_2(PO_4)_3$; 41.10 mg $CuTi_2(PO_4)_3$; and 32.08 mg $CuTiZr(PO_4)_3$ (as prepared by the method described above) using a Setaram TG-DTA 92 analyser. This was operated with a controlled atmosphere of artificial air; with $P_{O_2} = 0.2$ bar, and a gas flow rate = 42 mL/min. The samples were held inside small alumina crucibles. A full heating cycle was achieved by starting at room temperature, and increasing to 800 °C at a rate 0.5 °C/min; then immediately returning to room temperature at the same rate. A thermogravimetric analysis on the empty alumina crucible was used as the reference state for the purpose of internal thermal compensation; i.e., the *mass versus temperature* profile for the crucible was subtracted from the *mass versus temperature* profile for the sample and crucible.

Results and discussion

A set of powder X-ray diffraction patterns corresponding to the product materials in their reduced state: $CuZr_2(PO_4)_3$, $CuTi_2(PO_4)_3$ and $CuTiZr(PO_4)_3$, are shown in Figs. 3, 6 and 7, respectively. By comparing these powder patterns with the *powder diffraction files*™ (cf. the International

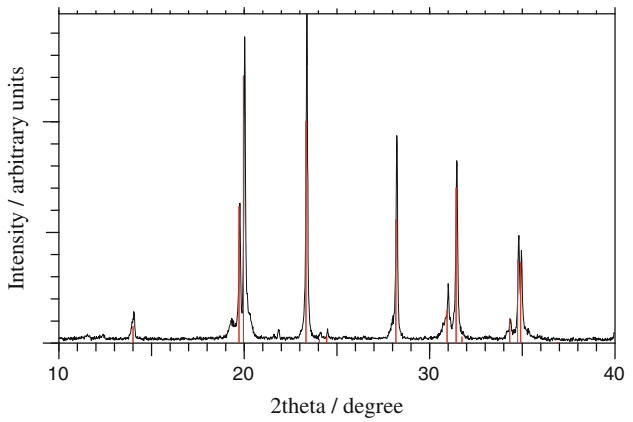

Fig. 3 Powder X-ray diffraction pattern (Cu $K_{\alpha 1}$ radiation) for $CuZr_2(PO_4)_3$ as prepared. PDF 81-527 $CuZr_2(PO_4)_3$ is shown in red for comparison

Table 1 Powder X-ray diffraction data for $CuTiZr(PO_4)_3$ indexed to a trigonal cell using the usual hexagonal coordinates (corresponding with Fig. 7)

2θ/°	*d*obs./Å	*I*/*I*1 obs.	*h k l*
14.28	6.190	6	1 0 2
20.13	4.407	24	1 0 4
20.45	4.339	72	1 1 0
23.88	3.724	100	1 1 3
25.05	3.553	5	2 0 2
28.84	3.093	42	2 0 4
31.72	2.818	16	2 1 1
32.12	2.784	49	1 1 6
35.05	2.557	8	1 0 8
35.60	2.520	15	2 1 4
35.78	2.507	18	3 0 0

Centre for Diffraction Data) PDF 81-527 and PDF 84-1355, it is apparent that the specimens of $CuZr_2(PO_4)_3$ and $CuTi_2(PO_4)_3$ have been prepared with a reasonably high degree of phase purity. With regard to the powder pattern for $CuTiZr(PO_4)_3$, a list of the observed *d*-values, with their relative intensities, is reported in Table 1. These peaks (marked as red lines in Fig. 7) were indexed to a rhombohedral lattice using a trigonal cell with the usual hexagonal coordinates. The few unmarked peaks in Fig. 7 are attributed to phase impurities. The corresponding hexagonal cell constants were determined as: $a = 8.686(1)$ Å and $c = 21.762(5)$ Å, with $Z = 6$ and the cell volume = 1421.8 $Å^3$. These cell constants lie centrally in between those for the two end-members: namely, $CuTi_2(PO_4)_3$ with $a = 8.523(2)$ Å and $c = 21.303(4)$ Å [18]; and $CuZr_2(PO_4)_3$ with $a = 8.9018(2)$ Å and $c = 22.2021(6)$ Å [14]; and are consistent with $CuTiZr(PO_4)_3$ being a midintermediate member of the solid solution.

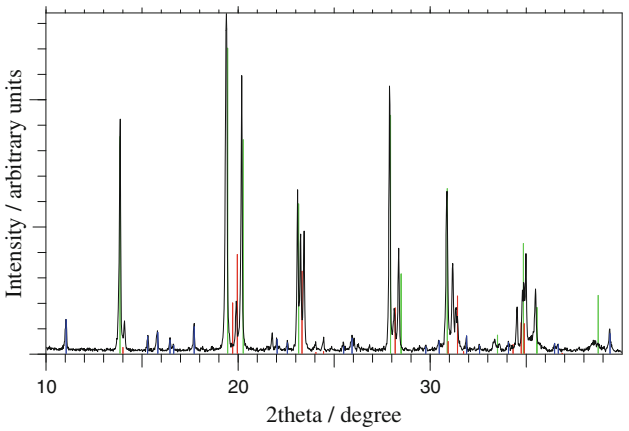

Fig. 4 Powder X-ray diffraction pattern (Cu $K_{\alpha 1}$ radiation) for the product material after oxidising $CuZr_2(PO_4)_3$ in air at 400 °C for 72 h. PDF 47-75 for $Cu_{0.5}Zr_2(PO_4)_3$ and PDF 81-527 for $CuZr_2(PO_4)_3$ are shown in *green* and *red*, respectively, for comparison. The remaining unmatched peaks are marked in *blue* (*see text*)

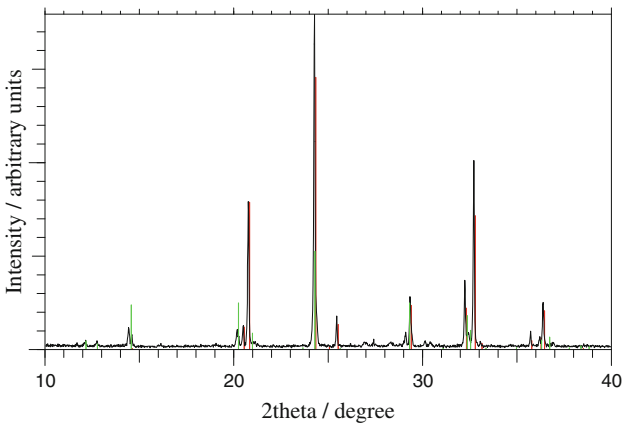

Fig. 5 Powder X-ray diffraction pattern (Cu $K_{\alpha 1}$ radiation) for the product material after oxidising $CuTi_2(PO_4)_3$ in air at 400 °C for 72 h. PDF 86-555 for $Cu_{0.5}Ti_2(PO_4)_3$ and PDF 84-1355 for $CuTi_2(PO_4)_3$ are shown in *green* and *red,* respectively, for comparison

Moreover, the ratio *c*/*a* for $CuTiZr(PO_4)_3$ is very similar to that for the two end-members. The cell constants reported for $CuTiZr(PO_4)_3$ in this present work differ significantly to the values; $a = 8.733(3)$ Å and $c = 22.042(30)$ Å as reported originally by Berry et al. [7] for this composition. These values by Berry et al. [6] have been edited subsequently in the corresponding PDF 48-659, so as to read: $a = 8.709$ Å and $c = 21.855$ Å. Nota bene Berry et al. [7] were unable to observe the peaks: (202), (116) and (118) in their powder pattern.

A set of powder X-ray diffraction patterns corresponding to the above materials *after* they had been subjected to oxidation in air at 400 °C for 72 h are shown in Figs. 4, 5 and 8. From Fig. 4, it is evident that $CuZr_2(PO_4)_3$ was almost completely oxidised to $Cu_{0.5}Zr_2(PO_4)_3$ under these conditions. The unmatched peaks as marked with blue lines

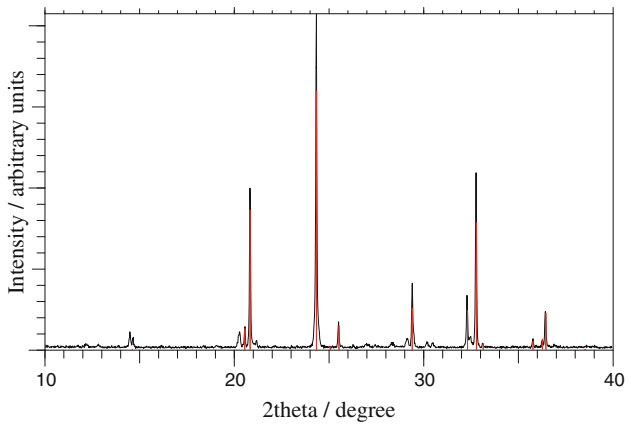

Fig. 6 Powder X-ray diffraction pattern (Cu $K_{\alpha 1}$ radiation) for $CuTi_2(PO_4)_3$ as prepared. PDF 84-1355 $CuTi_2(PO_4)_3$ is shown in *red* for comparison

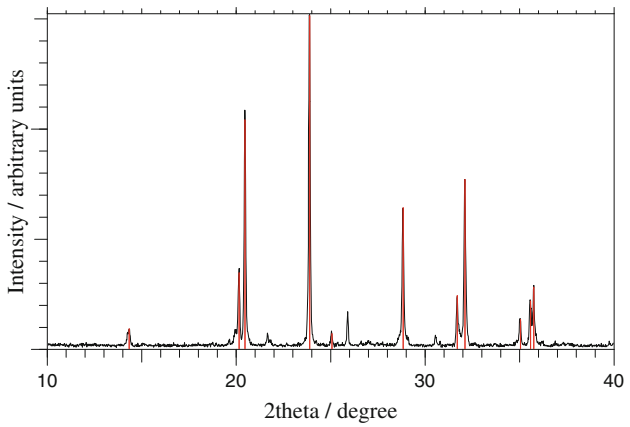

Fig. 7 Powder X-ray diffraction pattern (Cu $K_{\alpha 1}$ radiation) for $CuTiZr(PO_4)_3$ as prepared. The peaks marked in *red* are indexed and shown in Table 1

in Fig. 4, relate to an unidentified crystalline phase that is soluble in acid solution, and is apparently a very dark material. The mass balance of this system suggests that this phase is a form of copper oxide as formed in air at the relatively low temperature of 400 °C. But surprisingly, these peaks correspond neither to tenorite (CuO), paramelaconite (Cu_4O_3) nor, cuprite (Cu_2O). A minor amount of unreacted $CuZr_2(PO_4)_3$ was observed, however, in this powder pattern.

The powder pattern in Fig. 5, indicates that $CuTi_2(PO_4)_3$ has essentially survived the oxidising treatment at 400 °C. The low-angle peaks (with weak intensities) at: 12.2; 12.7; 14.6; and 20.2° 2θ correspond to the (003), (001), (102) and (104) lattice spacings as reported in the PDF 86-555 for rhombohedral $Cu_{0.5}Ti_2(PO_4)_3$. Interestingly, these peaks are also present (albeit with very weak intensities) in the precursor material (cf. Fig. 6), and suggest, likewise, that this material may be contaminated with a trace amount of $Cu_{0.5}Ti_2(PO_4)_3$. The observation that the material retains its reddish brown colouration throughout this treatment, is consistent with the material remaining as essentially, $CuTi_2(PO_4)_3$.

The powder pattern in Fig. 8, indicates clearly that $CuTiZr(PO_4)_3$ has undergone a partial oxidation during the oxidising treatment at 400 °C in air (72 h). Nearly all of the peaks can be matched with either, $CuTiZr(PO_4)_3$ (cf. Fig. 7) or, the newly characterised phase $Cu_{0.5}TiZr(PO_4)_3$ (cf. Fig. 9); thereby indicating the presence of both of these phases. Furthermore, this result is consistent with the change in the colouration of the powdered material; from orange-brown to medium grey.

Figure 9 shows the powder pattern of the product material in an attempt to oxidise $CuTiZr(PO_4)_3$ at 400 °C in pure oxygen (48 h) to yield $Cu_{0.5}TiZr(PO_4)_3$ as a single phase material. It is interesting to note that the precursor material $CuTiZr(PO_4)_3$ has been oxidised completely in this reaction, even though the duration of the reaction was shorter than the one performed in air (see above). This implies that the rate of this oxidation process is enhanced by an increase in the partial pressure of oxygen at a given temperature (viz. 400 °C); demonstrating that the rate is not limited by the Cu^+ mobility. A list of the observed *d*-values, with their relative intensities, is reported in Table 2. These values (marked as green lines in Fig. 9) were indexed to a rhombohedral lattice using a trigonal cell with the usual hexagonal coordinates. The few unmarked peaks in Fig. 9 are attributed to phase impurities. The corresponding hexagonal cell constants were determined as: $a = 8.599(1)$ Å and $c = 22.355(3)$ Å, with $Z = 6$ and the cell volume = 1431.6 Å^3. These cell constants lie centrally in between those for the two end-members:

Table 2 Powder X-ray diffraction data for $Cu_{0.5}TiZr(PO_4)_3$ indexed to a trigonal cell using the usual hexagonal coordinates (corresponding with Fig. 9)

2θ/°	*d*obs./Å	*I*/*I*1 obs.	*h k l*
11.84	7.466	4	0 0 3
12.49	7.081	5	1 0 1
14.25	6.212	51	1 0 2
19.82	4.477	97	1 0 4
20.61	4.305	66	1 1 0
23.84	3.730	100	1 1 3
28.75	3.103	57	2 0 4
31.73	2.818	50	1 1 6
31.99	2.796	18	2 1 1
34.21	2.619	4	1 0 8
35.65	2.517	18	2 1 4
36.11	2.486	25	3 0 0
37.71	2.384	4	2 1 5
38.16	2.356	5	3 0 3

namely, $Cu_{0.5}Ti_2(PO_4)_3$ with $a = 8.41 \pm 0.01$ Å and $c = 21.88 \pm 0.04$ Å [19]; and $Cu_{0.5}Zr_2(PO_4)_3$ with $a = 8.84 \pm 0.02$ Å and $c = 22.77 \pm 0.02$ Å [10]; and are consistent with $Cu_{0.5}TiZr(PO_4)_3$ being a midintermediate member of this particular solid solution. Moreover, the ratio *c*/*a* for $Cu_{0.5}TiZr(PO_4)_3$ is very similar to that for the two end-members.

These crystallographic measurements indicate that the phase transition from $CuTiZr(PO_4)_3$ to $Cu_{0.5}TiZr(PO_4)_3$ is accompanied by a very slight *increase* (+0.7%) in the volume of the unit cell. This implies that the $[TiZr(PO_4)_3]^-$ NASICON-type framework structure can tolerate a loss of 50% of the copper content of the material whilst remaining almost rigid. Therefore, the rearrangements in the valency, coordination and site occupation factors of the copper ions exert only a small change in the volume of the unit cell, whilst the ratio *c*/*a* increases from 2.51 to 2.56.

The powder specimen of $Cu_{0.5}TiZr(PO_4)_3$, as prepared in this work, displays a bright green colouration. This is consistent with the green material that was formed in the vicinity of the platinum anode during the electrochemical polarisation (at 300 °C under argon) of an orange-coloured ceramic monolith of $CuTiZr(PO_4)_3$, as reported by one of us previously [8]. This abrupt change in the colour of the ceramic material, from orange to green, was interpreted as an indication of immiscibility in the copper composition of this electrolyte; and it was suggested, at that time, that this green material was most likely to be the analogous cupric compound, $Cu_{0.5}TiZr(PO_4)_3$ [8]. The interpretation of the powder X-ray diffraction patterns as shown in Figs. 7, 8 and 9, strongly supports this earlier suggestion.

The results of the thermogravimetric analyses, as performed on the product materials that were initially in their reduced state: $CuZr_2(PO_4)_3$, $CuTi_2(PO_4)_3$ and $CuTiZr(PO_4)_3$, are shown in Figs. 10, 11 and 12, respectively. In general, these materials are considered to be metastable under ambient conditions (i.e., $P_{O_2} = 0.2$ bar and $T = 25$ °C). From Fig. 10, it can be seen that when $CuZr_2(PO_4)_3$ is heated in air from room temperature, it first undergoes an oxidation reaction that commences at ~300 °C to form a binary mixture of $Cu_{0.5}Zr_2(PO_4)_3$ and, presumably, CuO (cf. Fig. 4). This is followed by a reduction reaction that commences at ~510 °C, whereupon this material looses oxygen and reverts to single phase $CuZr_2(PO_4)_3$. During the cooling cycle, $CuZr_2(PO_4)_3$ begins to undergo oxidation at ~500 °C to form a binary mixture of $Cu_{0.5}Zr_2(PO_4)_3$ and, presumably, CuO. This cycle corresponds, in principle, to the reversible reaction:

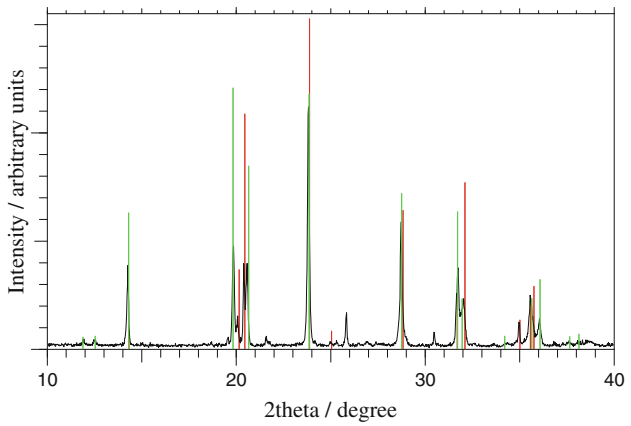

Fig. 8 Powder X-ray diffraction pattern (Cu $K_{\alpha 1}$ radiation) for the product material after oxidising $CuTiZr(PO_4)_3$ in air at 400 °C for 72 h. The peaks marked in *red* are indexed to $CuTiZr(PO_4)_3$ (cf. Table 1 and Fig. 7). The peaks marked in *green* are indexed to $Cu_{0.5}TiZr(PO_4)_3$ (cf. Table 2 and Fig. 9)

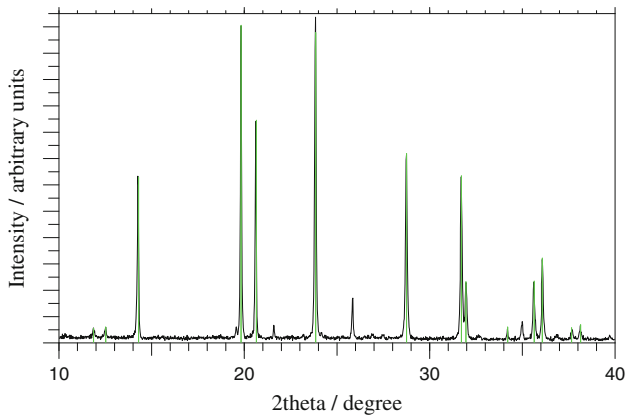

Fig. 9 Powder X-ray diffraction pattern (Cu $K_{\alpha 1}$ radiation) for the product material after oxidising $CuTiZr(PO_4)_3$ in oxygen at 400 °C for 48 h and, washing with dilute HNO_3 acid solution. The peaks marked in *green* are attributed to $Cu_{0.5}TiZr(PO_4)_3$; these are indexed and shown in Table 2

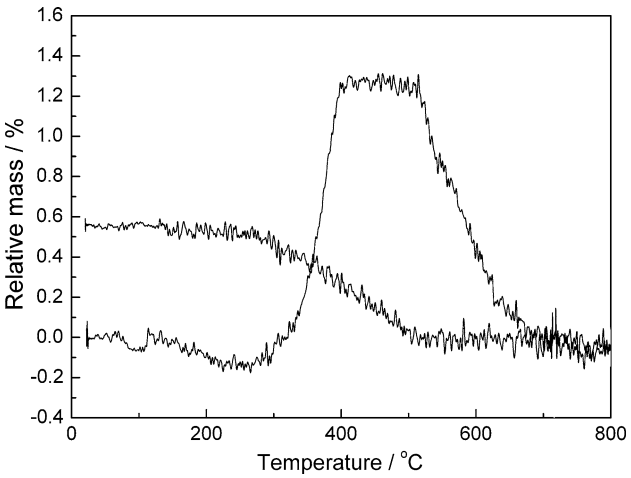

Fig. 10 Thermogravimetric hysteresis loop for $CuZr_2(PO_4)_3$ in artificial air ($P_{O_2} = 0.2$ bar), with heating and cooling rates of 0.5 °C/min

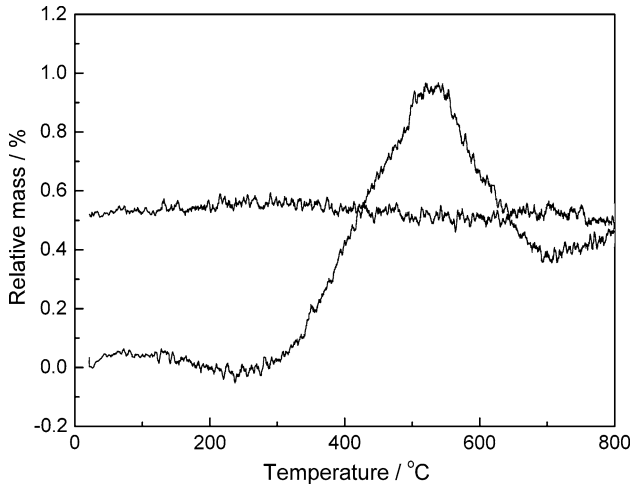

Fig. 11 Thermogravimetric hysteresis loop for $CuTi_2(PO_4)_3$ in artificial air ($P_{O_2} = 0.2$ bar), with heating and cooling rates of 0.5 °C/min

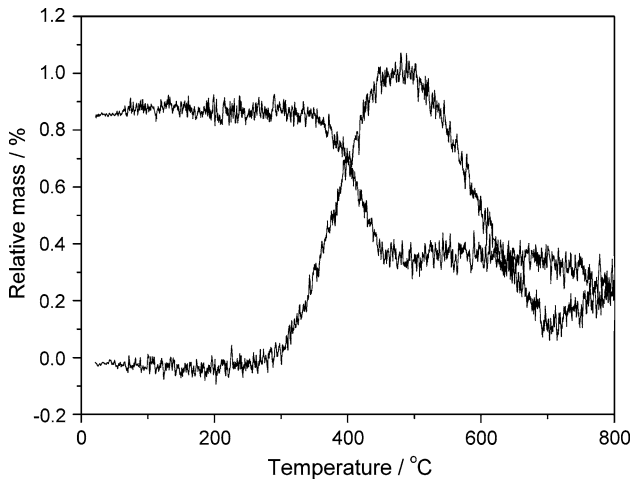

Fig. 12 Thermogravimetric hysteresis loop for $CuTiZr(PO_4)_3$ in artificial air ($P_{O_2} = 0.2$ bar), with heating and cooling rates of 0.5 °C/min

$$4Cu^{I}Zr_2(PO_4)_3 + O_2 \leftrightarrows 4Cu^{II}_{0.5}Zr_2(PO_4)_3 + 2Cu^{II}O$$

According to the above reaction, the theoretical increase in mass upon complete oxidation should correspond to 1.51%. However, the observed relative mass increase during the initial oxidation was only 1.25%; which suggests that this process is incomplete. Likewise, the oxidation during the cooling cycle is also incomplete. Alternatively, the possibility of forming the known oxygen deficient phases, cuprite, Cu_2O and metastable paramelaconite, Cu_4O_3 has been eliminated here through the results of powder X-ray diffractometry, as discussed above. From Fig. 11, it can be seen that $CuTi_2(PO_4)_3$ is oxidised much less effectively, with a mass increase of only 0.95%; compared with a theoretical maximum of 1.80%; whilst no oxidation is observed during the cooling cycle. From Fig. 12, the shape of the thermogravimetric loop for $CuTiZr(PO_4)_3$ lies in between these two extreme cases; with a mass increase of 1.00%; compared with a theoretical maximum of 1.64%.

The equilibrium temperature for this reduction/oxidation process is fairly constant across this solid solution, and occurs in the vicinity of 500 ± 25 °C (in air). This work has identified, however, that there are significant differences in the rate of oxidation, and that the rate is systematically dependent on the ratio of Ti/Zr within the material. Some of the reasons as to why titanium should exert such a large passivity are discussed below.

In general, the formation of the product layer during oxidation may cause an impediment to the mass transfer of copper and oxygen across the interfacial reaction boundary; but this aspect is considered to be similar for all three compositions. Another possibility is that the site occupation factors of the copper ions within the oxidised phosphate material may be influential in this system. Olazcuga et al. [19] consider that copper(II) ions occupy solely the M(2) site in $Cu_{0.5}Ti_2(PO_4)_3$ [19]; whereas, in $Cu_{0.5}Zr_2(PO_4)_3$ they are considered to be distributed over both the M(1) and M(2) sites, but with a preference for the M(1) site [20]. Hence, the oxidation of $CuTi_2(PO_4)_3$ to $Cu_{0.5}Ti_2(PO_4)_3$ is considered by Olazcuga et al. [19] to be accompanied by the migration of the copper ions from the M(1) site into the M(2) site. Whereas, during the oxidation of $CuZr_2(PO_4)_3$, there is the possibility that a large percentage of the newly formed copper(II) ions remain within the M(1) site. However, the ionic conductivities for these three materials are very similar to each other [8], and therefore, the mobility of the Cu^+ ion is unlikely to be the rate limiting factor in the especially sluggish chemical oxidation of $CuTi_2(PO_4)_3$ at elevated temperature (≥300 °C).

At present, it is only possible to speculate that the difference in their kinetic behaviour may be connected with the effect that substituting titanium(IV) for zirconium(IV) has on the electronic structure of this material; noting that Ti^{4+} ions are much more polarisable than Zr^{4+} ions. For example, El Jazouli et al. [9] suggested that the intense colouration of the titanium compound, $CuTi_2(PO_4)_3$, is a consequence of the charge transition: $Cu^+(3d^{10}) + Ti^{4+}(3d^0) \rightarrow Cu^{2+}(3d^9) + Ti^{3+}(3d^1)$. If so, then depending on the time-frame, this reduced phase can be perceived momentarily as, $Cu^{2+}Ti^{3+}Ti^{4+}(PO_4)_3$; such that the charge transfer mechanism for its oxidation by dioxygen (O_2) molecules may be quite different to that for $Cu^+Zr^{4+}Zr^{4+}(PO_4)_3$, and controlled perhaps by a surface reaction. These aspects must surely be important in the role of $CuTi_2(PO_4)_3$ as a catalyst.

Conclusion

$CuTiZr(PO_4)_3$ and $Cu_{0.5}TiZr(PO_4)_3$ have been prepared and structurally characterised using powder X-ray diffractometry. The latter, confirms the existence of $Cu_{0.5}TiZr(PO_4)_3$. This work has shown that even though the compounds: $CuTi_2(PO_4)_3$, $CuTiZr(PO_4)_3$ and $CuZr_2(PO_4)_3$ are part of the same solid solution series, and appear to exhibit a similar thermodynamic stability under oxidising conditions (with respect to their copper(II) analogues and CuO), there is a remarkable difference in the kinetics for their chemical oxidation. The results of powder X-ray diffractometry and thermogravimetric analysis performed on samples of these materials under oxidising conditions in air, demonstrate that the substitution of titanium(IV) for zirconium(IV) results in a greater passivity to chemical oxidation, whilst not adversely affecting their ionic conducting properties in the cuprous state. This feature is of importance for the technological exploitation of this material as a solid electrolyte and, presumably, also as a catalyst.

This work has shown that $CuTi_2(PO_4)_3$ is much more passive to chemical oxidation than $CuZr_2(PO_4)_3$. Therefore, $CuTi_2(PO_4)_3$ offers a clear advantage over $CuZr_2(PO_4)_3$ when being considered for use as a Cu^+ solid electrolyte below 525 °C in air. In the past, the deep reddish brown colouration of $CuTi_2(PO_4)_3$ may have hindered the use of this material as a copper(I) solid electrolyte, due to the common association of darkly coloured materials with electronic conductivity. This prejudice should be put aside, to some extent, when evaluating the technological exploitation of this material in the light of the results presented in this present article.

The authors are presently attempting to identify and characterise more fully the dark-coloured copper oxide phase formed during the oxidation of $CuZr_2(PO_4)_3$ under air at 400 °C. These findings will be reported in due course.

Acknowledgements The authors are grateful to Professor Andrew Bond for assistance with indexing the powder X-ray diffraction patterns for $CuTiZr(PO_4)_3$ and $Cu_{0.5}TiZr(PO_4)_3$.

References

1. Hong HY-P (1976) Mater Res Bull 11:173
2. Yao PC, Fray DJ (1983) Solid State Ionics 8:35
3. Davidson AJ, Fray DJ (2000) Solid State Ionics 136–137:613
4. Oudet F, Vejux A, Kompany T, Bordes E, Courtine P (1989) Mater Res Bull 24:561
5. Kousuke Y, Yoshihiro A (2000) Mater Res Bull 35:211
6. Mbandza A, Bordes E, Courtine P (1985) Mater Res Bull 20:251
7. Berry FJ, Oates G, Smart LE, Vithal M, Cook R, Ricketts HG, Williams R, Marco JF (1992) Polyhedron 11:2543
8. Warner TE, Milius M, Maier J (1992) Ber Bunsenges Phys Chem 96:1607
9. Jazouli AE, Soubeyroux JL, Dance JM, Flem GL (1986) J Solid State Chem 65:351
10. Jazouli AE, Alami M, Brochu R, Dance JM, Flem GL, Hagenmuller P (1987) J Solid State Chem 71:444
11. Polles GL, Jazouli AE, Olazcuaga R, Dance JM, Flem GL, Hagenmuller P (1987) Mater Res Bull 22:1171
12. Bussereau I, Olazcuaga R, Flem GL, Hagenmuller P (1989) Eur J Solid State Inorg Chem 26:383
13. Christensen E, Barner JH, Engell J, Bjerrum HJ (1990) J Mater Sci 25:4060. doi:10.1007/BF00582482
14. Bussereau I, Belkhiria MS, Gravereau P, Boireau A, Soubeyroux JL, Olazcuagal R, Flem GL (1992) Acta Cryst C 48:1741
15. Christensen RH-W, Warner TE (2006) J Mater Sci 41:1197. doi:10.1007/s10853-005-3657-1
16. Warner TE, Edwards PP, Fray DJ (1991) Mater Sci Eng B8:219
17. Boultif A, Louer D (2004) J Appl Cryst 37:724
18. McCarron EM, Calabrese JC, Subramanian MA (1987) Mater Res Bull 22:1421
19. Olazcuaga R, Flem GL, Boireau A, Soubeyroux JL (1994) Adv Mater Res 1:177
20. Taoufik I, Haddad M, Nadiri A, Brochu R, Berger R (1999) J Phys Chem Solids 60:701
21. Mbandza A, Bordes E, Courtine P, Jazouli AE, Soubeyroux JL, Flem GL, Hagenmuller P (1988) React Solid 5:315